

# Vulnerability Analysis of Safe Reinforcement Learning via Inverse Constrained Reinforcement Learning

Jiali Fan<sup>1</sup>, Shixiong Jiang<sup>1</sup>, Mengyu Liu<sup>2</sup>, Fanxin Kong<sup>1</sup>

<sup>1</sup>University of Notre Dame

<sup>2</sup>Washington State University Tri-Cities

{jfan5, sjiang5, fkong}@nd.edu, mengyu.liu@wsu.edu

## Abstract

Safe reinforcement learning (Safe RL) aims to ensure policy performance while satisfying safety constraints. However, most existing Safe RL methods assume benign environments, making them vulnerable to adversarial perturbations commonly encountered in real-world settings. In addition, existing gradient-based adversarial attacks typically require access to the policy’s gradient information, which is often impractical in real-world scenarios. To address these challenges, we propose an adversarial attack framework to reveal vulnerabilities of Safe RL policies. Using expert demonstrations and black-box environment interaction, our framework learns a constraint model and a surrogate (learner) policy, enabling gradient-based attack optimization without requiring the victim policy’s internal gradients or the ground-truth safety constraints. We further provide theoretical analysis establishing feasibility and deriving perturbation bounds. Experiments on multiple Safe RL benchmarks demonstrate the effectiveness of our approach under limited privileged access.

## 1 Introduction

Safe reinforcement learning (Safe RL) integrates safety constraints into policy optimization, enabling agents to balance performance with safety requirements [Gu *et al.*, 2022]. Owing to its ability to enforce safety during training and deployment, Safe RL has been widely applied in safety-critical domains, including autonomous driving and robotic manipulation.

However, most existing Safe RL methods assume benign, attack-free environments, leaving them vulnerable to adversarial perturbations that frequently occur in the real world.

Traditional adversarial attack methods [Goodfellow *et al.*, 2014; Madry *et al.*, 2018; Lin *et al.*, 2017] for RL aim to downgrade the reward/performance of the agent, rather than safety violations. Recent studies have investigated this vulnerability by designing adversarial attacks targeting the observation space of trained Safe RL agents [Liu *et al.*, 2022b; Jiang *et al.*, 2024]. While insightful, these approaches typically rely on strong assumptions such as access to the pol-

icy’s internal gradients [Liu *et al.*, 2022b] or knowledge of the ground-truth safety constraints [Jiang *et al.*, 2024], which limits their applicability in practical attack scenarios.

These limitations raise a fundamental question: *Can we systematically reveal and evaluate the safety vulnerabilities of Safe RL policies in a practical setting without requiring privileged access to the victim’s gradients or the ground-truth constraints?* Addressing this problem poses several key challenges. First, current effective adversarial attacks are gradient-based and require access to victim’s gradients to guide the attack. Second, how can we ensure that adversarial inputs result in actual safety violations instead of simply lowering performance or rewards? Third, how can we determine an attack strength that leads to safety violations without compromising stealth?

To tackle these challenges, we propose an adversarial attack framework based on inverse constrained reinforcement learning (ICRL) for Safe RL policies. Instead of using the policy’s internal gradients or safety constraints to generate adversarial perturbations, our method leverages ICRL to learn the safety constraints and a learner policy from expert demonstrations. Then, the learned constraints and learner policy are used to generate adversarial perturbations that cause higher cost values of safety constraint violations. Also, the learned constraints provide a theoretical bound on perturbations to estimate the optimal attack strength.

In summary, our contributions are as follows:

1. We propose a practical, demonstration-based adversarial analysis framework for Safe RL that learns constraints and a surrogate policy via ICRL using black-box environment interaction, enabling gradient-based attacks without privileged access to victim gradients or ground-truth constraints.
2. We provide theoretical analysis establishing the feasibility of the proposed framework and deriving bounds on attack effectiveness under limited knowledge assumptions.
3. We conduct extensive evaluations across multiple Safe RL benchmarks, demonstrating consistent safety violations under constrained perturbation budgets and offering insights into the vulnerabilities of different Safe RL algorithms.

## 2 Related Work

**Safe Reinforcement Learning (Safe RL).** Safe RL aims to ensure policy performance while satisfying safety constraints, which are increasingly applied in safety-critical applications, such as autonomous driving [Wachi *et al.*, 2024] and CPS [Bui *et al.*, 2024]. Lagrange-based Safe RL methods [Ray *et al.*, 2019; Stooke *et al.*, 2020] formulate safety constraints as penalties in the reward function using Lagrange multipliers to balance reward maximization and constraint satisfaction. [Ji *et al.*, 2024] developed a comprehensive Safe RL benchmark, OmniSafe, which includes a suite of Safe RL algorithms, a Gymnasium-like API, and a diverse set of safety-critical environments. [Brunke *et al.*, 2022] provides a systematic review of Safe RL methods in robotics, discussing different levels of safety and summarizing the corresponding technical approaches.

**Adversarial attacks on RL.** [Goodfellow *et al.*, 2014] first proposed the gradient-based adversarial attack method, fast gradient sign method (FGSM), for neural network-based policies. Further, [Huang *et al.*, 2017] extends FGSM to RL algorithms. Additionally, defense methods have been proposed to enhance policy robustness. For instance, [Liang *et al.*, 2022] introduces a robust training framework to optimize reward when the policy is under adversarial attack. [Zhang *et al.*, 2020] introduces state-adversary Markov Decision Process (SA-MDP) for robustness improvement of RL algorithms.

There are also some works on adversarial attacks on Safe RL policies. [Liu *et al.*, 2022b] proposed an approach targeting Safe RL policies to manipulate the gradient of the reward critic and safety critic to violate safety constraints. However, this method requires the policy’s gradient information. [Jiang *et al.*, 2024] introduced an adversarial attack method on Safe RL systems, which is guided by robustness values derived from the quantitative semantics of STL. However, it assumes prior knowledge of the system’s safety constraints.

**Safety Constraint Mining and Inference in RL.** A growing body of work aims to infer unknown safety constraints directly from system interactions or observed behaviors, without requiring explicit access to the underlying specifications. Existing approaches differ in how constraints are represented, ranging from symbolic rules to implicit, data-driven models learned from trajectories. Within this topic, two prominent paradigms are STL mining and ICRL. STL mining represents a symbolic approach to safety constraint mining, where safety requirements are expressed as temporal logic specifications inferred from system trajectories. For example, recent work [Yifru and Baheri, 2024] jointly learns a safe RL policy and unknown safety constraint parameters by optimizing parametric STL specifications over interaction data, demonstrating that mined STL constraints can closely approximate true environmental safety boundaries.

In contrast, ICRL aims to infer safety constraints implicitly from expert demonstrations or constrained interactions. Scobee et al. [Scobee and Sastry, 2019] extended MaxEnt IRL to constrained settings to recover latent safety constraints from expert behavior. Subsequent learning-based ICRL methods represent constraints using neural network classifiers or cost functions, enabling extensions to stochas-

tic, multi-task, and multi-modal environments [Malik *et al.*, 2021; McPherson *et al.*, 2021; Kim *et al.*, 2024; Lindner *et al.*, 2024; Qiao *et al.*, 2024]. Benchmarking efforts and theoretical connections to standard IRL have also been explored [Liu *et al.*, 2022a; Hugessen *et al.*, 2024], along with robust variants that address environment mismatch and real-world uncertainty [Xu and Liu, ]. Overall, ICRL learns safety constraints as continuous, differentiable functions, avoiding predefined logical templates and scaling naturally to high-dimensional, nonlinear systems, at the cost of reduced interpretability.

## 3 Problem Formulation

### 3.1 Safe Reinforcement Learning

Safe RL integrates safety constraints into the policy learning process, ensuring that the policy not only maximizes expected rewards but also adheres to predefined safety requirements. The problem is typically formulated as a Constrained Markov Decision Process (CMDP), represented as  $(S, A, r, c, p, \gamma)$ , where  $S$  is the state space;  $A$  is the action space;  $r : S \times A \times S \rightarrow \mathbb{R}$  denotes the reward function;  $c : S \times A \times S \rightarrow \mathbb{R}^+$  denotes the cost function for safety constraint violations;  $p : S \times A \times S \rightarrow [0, 1]$  is the transition probability function; and  $\gamma \in [0, 1]$  is the discount factor. The objective of Safe RL is to maximize the expected cumulative reward while ensuring that the expected cost remains below a predefined threshold  $d$ , formally expressed as:

$$\pi^* = \arg \max_{\pi} V_r^{\pi}, \quad \text{s.t.} \quad V_c^{\pi} \leq d, \quad (1)$$

where  $V_r^{\pi}$  denotes the expected cumulative reward under policy  $\pi$ , and  $V_c^{\pi}$  denotes the expected cumulative cost. Various algorithms extend traditional RL methods to address such constrained optimization problems, including PPO-Lagrangian [Ray *et al.*, 2019] and PID-Lagrangian-TRPO [Stooke *et al.*, 2020].

### 3.2 Threat Model

**Attack Setup:** We consider adversarial attacks on an expert policy  $\pi_E$  trained by a safe RL algorithm. At each time step  $t$ , the attacker adds a perturbation  $\delta_t$  to the agent’s observation  $s_t$ , yielding a modified input  $\hat{s}_t = s_t + \delta_t$ . The expert policy then selects an action  $\hat{a}_t = \pi_E(\hat{s}_t)$ , which drives the environment transition  $s_{t+1} = p(s_{t+1} | s_t, \hat{a}_t)$ . The attacker applies such perturbations throughout the episode.

#### Attacker’s Capability:

- The attacker can perturb observations  $s_t$  within a norm-bounded region:  $\|\delta_t\| \leq \epsilon$ , where  $\epsilon$  is a user-defined attack budget.
- The attacker does not modify the environment dynamics, rewards, or constraints directly.

#### Adversarial Knowledge:

The practical threat model:

- The attacker has **no access** to the gradient information of  $\pi_E$ .
- The attacker does **not know** the environment’s true reward or constraint functions.

Table 1: Access levels for adversarial attacks on Safe RL. Lower levels require less privileged access (more stealthy). Environment interaction is orthogonal and reported separately.

Level	Access Assumption	Privileged Access
L1	Trajectories + black-box interaction;	None
L2	Trajectories + partial privileged info (safety constraints <i>or</i> gradients)	Partial
L3	Trajectories + full privileged info (safety constraints + gradients)	Full

- The attacker can collect a **limited number of expert trajectories**  $\mathcal{D}_E = \{\tau_i\}_{i=1}^N$ , where each trajectory  $\tau_i = \{(s_t, a_t, r_t)\}_{t=0}^T$ .
- The attacker may perform **black-box interaction** (black-box rollouts) with the environment to train surrogate models (learner policy and constraint network) via ICRL; this interaction does not require access to victim parameters.

**Note.** In benchmark environments, we compute ground-truth violations during evaluation using the environment’s constraint checker (not the learned constraint network). In real-world systems where constraints are not observable, the attacker relies on demonstrations and black-box interaction only.

### 3.3 Attack Metrics

We make the following definitions and assumptions for the adversarial attack on Safe RL.

**Attack Effectiveness:** We define an adversarial attack on the expert policy  $\pi_E$  as effective if introducing a perturbation  $\delta$  increases the constraint violation cost relative to the original (unperturbed) scenario. Formally, this effectiveness condition can be expressed as:  $V_c^{\pi_E^\psi}(s + \delta) > V_c^{\pi_E^\psi}(s)$ , where  $V_c^{\pi_E^\psi}(s + \delta)$  represents the cumulative constraint violation cost when the policy input state  $s$  is perturbed by  $\delta$ .

**Attack Strength:** The strength of an adversarial attack is characterized by the magnitude of the perturbation applied to the input state. It is quantified by the  $L_\infty$ -norm of the difference between the original state  $s$  and the perturbed state  $\tilde{s}$ , constrained by the attack budget  $\epsilon$ :  $\|\tilde{s} - s\|_\infty \leq \epsilon$ , where  $\epsilon$  controls the maximum allowable deviation and thus determines the strength and subtlety of the attack.

**Attack Stealthiness:** We define stealthiness with respect to *privileged access*—attacks requiring less privileged information (e.g., victim gradients, ground-truth constraints) are considered more stealthy. Environment interaction is treated as a separate dimension. Table 1 summarizes the access levels; our method (L1) avoids privileged access while allowing black-box queries.

In experiments, we report (i) episodic cumulative cost, (ii) violation rate (percentage of episodes with cost exceeding the environment’s cost limit), and (iii) episodic return.

### 3.4 Learning Constraints via ICRL

ICRL [Kim *et al.*, 2024] assumes that the safety constraints of the environment are unobservable or difficult to formulate mathematically. It aims to learn the safety constraint function  $\psi$  from expert demonstrations. One representative ICRL method is using contrastive learning to learn a neural network discriminator by distinguishing the expert demonstrations from the learner demonstrations. It consists of two steps: constrained RL policy (learner policy) learning and safety constraint learning. The learner policy learning aims to learn a policy that has task reward as close as the expert policy, as well as keeping the costs of safety violation no more than the expert policy. It can be formulated as a min-max problem:

$$\begin{aligned} & \min_{\pi_L \in \Pi} V_r^{\pi_E} - V_r^{\pi_L} \\ & \text{s.t. } \max_{\psi \in \mathcal{F}_\psi} \left( V_c^{\pi_L^\psi} - V_c^{\pi_E^\psi} \right) \leq 0, \end{aligned} \quad (2)$$

where  $\pi_L$  represents learner policy;  $V_r^{\pi_L}$  and  $V_r^{\pi_E}$  are the expected cumulative reward under  $\pi_L$  and  $\pi_E$ ;  $\mathcal{F}_\psi$  is the set of all possible constraints;  $V_c^{\pi_L^\psi}$  is the expected cumulative cost under  $\pi_L$  and constraint function  $\psi$ ;  $V_c^{\pi_E^\psi}$  is the cumulative cost of the expert policy  $\pi_E$  under the learned constraint  $\psi$ . The second step is to learn the safety constraint function  $\psi$  from expert demonstrations by identifying behavioral differences between the expert and the learner. To do so, we optimize for a constraint function that maximally separates the expert policy  $\pi_E$  from the set of previously learned learner policies  $\{\pi_{Lj}\}_{j=1}^T$ . The optimization objective is formulated as

$$\psi \leftarrow \arg \max_{\psi \in \mathcal{F}_\psi} \sum_{j=1}^T \left[ V_c^{\pi_{Lj}^\psi} - V_c^{\pi_E^\psi} \right] - R(\psi), \quad (3)$$

where  $V_c^{\pi_{Lj}^\psi}$  is the expected cumulative cost under policy  $\pi_{Lj}^\psi$ ;  $R(\psi)$  is the regularization term, instantiated as the  $L_2$ -norm in practice to prevent overfitting. Equation 3 encourages the learned constraint to penalize the learner’s behavior more than the expert’s, capturing implicit constraints obeyed by the expert demonstrations.

Finally, we can get a constraint function  $\psi$  and a learner policy  $\pi_L$  from the ICRL process.

## 4 Method

In this section, we introduce our proposed adversarial attack method based on the ICRL framework described in Section 3.4. An overview of the proposed method is shown in Figure 1.

### 4.1 Attack Generation

We leverage the learned constraint function  $\psi$  and the learner policy  $\pi$  to craft perturbations on the expert policy  $\pi_E$ . As defined in Section 3.3, our goal is to generate perturbations in the observation space that induce higher costs. Specifically, given the current observation  $s_t$ , we construct a perturbation  $\delta_t$  such that the adversarial action  $a'_t = \pi_L(s_t + \delta_t)$ , when propagated through the estimated one-step system dynamics

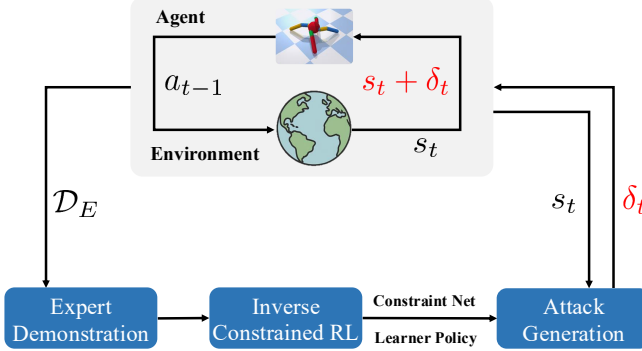


Figure 1: An overview of the proposed adversarial attack framework.

### Algorithm 1 Attack Generation

**Input:** Learner policy  $\pi_L$ , system identification function  $\hat{f}$ , constraint function  $\psi$ , expert policy's observation  $s_t$ , perturbation bound  $\epsilon$ , number of iterations  $n$ , step size  $\kappa$   
**Output:** Perturbation  $\delta_t$

```

1:  $s'_t \leftarrow s_t$  {Initialize perturbed state}
2: for  $i = 1$  to  $n$  do
3:    $a'_t \leftarrow \pi(s'_t)$  {Use learner policy to generate action}
4:    $\text{cost\_grad} \leftarrow \nabla_{s'_t} \psi(\hat{f}(s'_t, \pi_L(s'_t)))$  {Compute gradient}
5:    $s'_t \leftarrow s'_t + \kappa \cdot \epsilon \cdot \text{sign}(\text{cost\_grad})$  {Gradient ascent}
6:    $s'_t \leftarrow \max(\min(s'_t, s_t + \epsilon), s_t - \epsilon)$  {Clip}
7: end for
8:  $\delta_t \leftarrow s'_t - s_t$  {Compute final perturbation}
9: return  $\delta_t$ 

```

$\hat{f}$ , drives the system to the next state  $s'_{t+1} = \hat{f}(s_t, a'_t)$  that violates the learned safety constraints. Formally, the adversarial objective is defined as

$$\max_{|\delta_t| \leq \epsilon} \psi(f(s_t, \pi(s_t + \delta_t))), \quad (4)$$

where  $\epsilon$  denotes the attack strength.

Next, to address this optimization problem, we employ a first-order approximation method to efficiently compute adversarial perturbations under norm constraints. Firstly, the next state  $s_{t+1}$  is estimated through the function  $\hat{f}$ , obtained from a multi-layer perceptron (see Appendix 9.1 for details). Then, to check whether  $s_{t+1}$  violates the safety constraint, we use the cost function  $\psi$  learned by ICRL to output the estimated cost value of  $s_{t+1}$ . Since our goal is to generate the perturbation  $\delta_t$  to make the cost value as high as possible, we then use the gradient-based method to maximize the cost value. In the meantime, the perturbation is calculated by the gradient of the cost function and applied to the current state  $s_t$ . This process will be repeated until reaching the maximum number of iterations  $n$ . The final perturbation  $\delta_t$  is computed as the difference between the original state  $s_t$  and the perturbed state  $s'_t$ . The detailed attack generation process is shown in Algorithm 1.

### Algorithm 2 ICRL-Guided Attack Pipeline Against Victim Policy

**Input:** Victim policy  $\pi_E$ , expert demonstrations  $\mathcal{D}_E$ , attack budget  $\epsilon$ , step size  $\kappa$ , iterations  $n$

**Output:** Attacked rollouts and episode-level safety violation metrics

```

1: Train ICRL using  $\mathcal{D}_E$  and black-box environment interaction to obtain:
2:   learned constraint network  $\psi$  and surrogate learner policy  $\pi_L$ 
3: Train a differentiable dynamics model  $\hat{f}$  from  $\mathcal{D}_E$ 
4: for each evaluation episode do
5:   Reset environment and obtain initial state  $s_0$ 
6:   for  $t = 0$  to  $T - 1$  do
7:     Compute perturbation  $\delta_t$  by Algorithm 1 using  $(s_t, \pi_L, \hat{f}, \psi, \epsilon, \kappa, n)$ 
8:     Apply perturbation to victim observation:  $\hat{s}_t = s_t + \delta_t$ 
9:     Execute victim policy action:  $a_t = \pi_E(\hat{s}_t)$ 
10:    Step environment:  $s_{t+1} \sim p(\cdot | s_t, a_t)$ 
11:   end for
12:   Compute and store episode metrics (return, cost, violation flag)
13: end for

```

## 4.2 End-to-end attack pipeline

Algorithm 2 summarizes the complete attack procedure against the victim safe RL policy  $\pi_E$ . Our key idea is to leverage surrogate models learned via ICRL, namely the constraint network  $\psi$  and the learner policy  $\pi_L$ , to compute adversarial perturbations without requiring privileged access (e.g., gradients) from  $\pi_E$ . At each time step, the perturbation  $\delta_t$  is obtained by solving a constrained optimization problem using the surrogate models, which is implemented by the iterative projected update in Algorithm 1. The resulting perturbed observation is then fed into the victim policy  $\pi_E$  for action execution and environment rollout.

**Note.** The perturbation  $\delta_t$  is optimized using gradients from the surrogate models  $(\pi_L, \hat{f}, \psi)$ , while the victim policy  $\pi_E$  is treated as a black box and is only queried for action execution.

## 4.3 Theoretical Analysis of Adversarial Attack

**Validity of the Learned Constraint Function.** Our attack framework builds upon the inverse constrained reinforcement learning (ICRL) paradigm proposed by [Kim *et al.*, 2024], in which the constraint function  $\psi$  is recovered from expert demonstrations using a no-regret online learning algorithm (FTRL). According to Theorem 3.1 in [Kim *et al.*, 2024], there exists an iterate  $\psi$  such that the policy  $\pi_L^\psi$  optimized under  $\psi$  is  $\xi$ -approximately constrained-optimal, satisfying:

$$V_c^{\pi_L^\psi} - V_c^{\pi_E^\psi} \leq \xi \quad \text{and} \quad V_r^{\pi_L} \geq V_r^{\pi_E}. \quad (5)$$

This implies that the learned constraint function  $\psi$  approximates the ground-truth constraint function  $\psi^*$  asymptotically. As a result, optimizing under  $\psi$  yields a policy that weakly Pareto-dominates the expert policy, meaning that the learned

policy achieves at least as high a reward as the expert policy  $\pi_E$  while satisfying the constraint approximately, up to a small violation  $\xi$ .

**Theorem 1 (Feasibility of Constraint-Based Perturbations).** *Let  $\psi(s, a)$  be a constraint function learned via ICRL that satisfies  $\forall(s, a), |\psi(s, a) - \psi^*(s, a)| \leq \xi$ , where  $\psi^*$  denotes the ground-truth constraint. Let  $\pi_E$  be the expert policy, and let  $\delta$  be a perturbation such that  $\psi(s + \delta, \pi_E(s + \delta)) > \eta$ , where  $\eta$  is the violation threshold. Then, if  $\eta > \xi$ , we have  $\psi^*(s + \delta, \pi_E(s + \delta)) > \eta - \xi$ , i.e., the perturbed state-action pair also violates the true constraint up to a bounded approximation error.*

Intuitively, Theorem 1 shows that adversarial perturbations based on the learned constraint effectively induce real constraint violations, provided the approximation error is small. The proof is provided in Appendix 8.1.

**Lemma 1 (Local Optimality of Gradient-Based Attacks).** *Let  $\psi(s, a)$  denote the learned constraint function, and consider an adversarial perturbation  $\delta$  on the state  $s$  with magnitude bounded by  $\epsilon$ , i.e.,  $\|\delta\| \leq \epsilon$ . Define the optimization problem of maximizing constraint violation as:*

$$\max_{\|\delta\| \leq \epsilon} \psi(s + \delta, \pi_E(s + \delta)).$$

*The perturbation generated by projected gradient ascent:*

$$\delta^* = \epsilon \cdot \frac{\nabla_s \psi(s, \pi_E(s))}{\|\nabla_s \psi(s, \pi_E(s))\|}$$

*is a locally optimal solution to this optimization problem.*

Lemma 1 ensures the local optimality of our gradient-based adversarial perturbations, validating our attack's theoretical effectiveness. The proof is provided in Appendix 8.2.

**Lemma 2 (One-Step Perturbation Cost Value Bound).** *Assume that the constraint function  $\psi(s, a)$  is  $L_\psi$ -Lipschitz continuous with respect to state  $s$ , i.e., for all states  $s$ , actions  $a$ , and perturbations  $\delta$ , it holds that*

$$|\psi(s + \delta, a) - \psi(s, a)| \leq L_\psi \|\delta\|.$$

*Then, for any one-step perturbation  $\delta$  with  $\|\delta\| \leq \epsilon$ , we have the following upper bound on the perturbed constraint value:*

$$\psi(s + \delta, \pi_E(s + \delta)) \leq \psi(s, \pi_E(s)) + L_\psi \epsilon.$$

Lemma 2 provides an explicit upper bound on the increase in constraint violation caused by a single-step perturbation. The proof is provided in Appendix 8.3.

**Remark 1.** Compared to existing gradient-based adversarial attacks, which typically require explicit knowledge of the victim's policy or system dynamics to estimate theoretical bounds, our ICRL-based attack benefits from directly estimating the Lipschitz constant through the learned constraint network, thereby allowing **precise quantification** of attack strength and effectiveness.

**Lemma 3 (Episodic Perturbation Cost Value Bound).** *Consider an episode of length  $T$  with states  $\{s_t\}_{t=1}^T$  generated by expert policy  $\pi_E$ . Assume that the constraint function  $\psi(s, a)$  is  $L_\psi$ -Lipschitz continuous with respect to state*

*$s$ , and the system dynamics under  $\pi_E$  and perturbations are Lipschitz continuous with constant  $L_f$ . If a perturbation  $\delta_t$  with  $\|\delta_t\| \leq \epsilon$  is applied at each step  $t$ , the cumulative constraint cost over the episode satisfies:*

$$\begin{aligned} \sum_{t=1}^T \psi(s_t + \delta_t, \pi_E(s_t + \delta_t)) &\leq \sum_{t=1}^T \psi(s_t, \pi_E(s_t)) \\ &\quad + \frac{L_\psi \epsilon (1 - (L_f)^T)}{1 - L_f}. \end{aligned}$$

Lemma 3 extends this result by establishing a cumulative upper bound on constraint violation over an entire episode with sequential perturbations. The proof is provided in Appendix 8.4.

In summary, this section provided theoretical validation, optimality analysis, and explicit bounds for our ICRL-based adversarial attack framework.

## 5 Experiments

This section evaluates whether our framework can systematically induce ground-truth safety violations without privileged access (L1), and how it compares to stronger-assumption baselines (L2/L3).

### 5.1 Experimental Setup

We evaluate our method on four safe RL tasks from PyBullet-based environments [Ellenberger, 2018 2019], covering different agent morphologies and constraint types. Expert agents were trained using PPO-Lagrangian [Stooke *et al.*, 2020]. The environments are:

**Safe-Ant-Velocity:** The agent is an Ant robot tasked with moving forward along the positive  $x$ -axis. A velocity constraint restricts excessive or abrupt movements:  $\|q_{t+1} - q_t\|_2 / dt \leq 0.75$ , where  $q_t$  denotes the position at time  $t$ . Cost limit is set to 20.

**Safe-Ant-Position:** A position constraint is imposed on the Ant agent to restrict unsafe movements:  $0.5x_t - y_t \leq 0$ , where  $x_t, y_t$  denote the coordinates at time  $t$ . Cost limit is set to 100.

**SafetyBallRun:** A spherical Ball robot runs along the positive  $x$ -axis as fast as possible. Two constraints are applied: (i) boundary constraint  $|y| \leq 2.0$ , and (ii) velocity constraint  $\|v_{xy}\| \leq 2.5$  m/s. Cost is triggered when either constraint is violated.

**SafetyBallCircle:** A spherical Ball robot moves in a circular trajectory. The agent must stay within a circular boundary while following the circular path. The safety constraint penalizes deviations from the safe region, with cost triggered when the agent moves outside the designated circular boundary.

Table 2 summarizes the expert policy performance across all four environments. The results indicate that the expert policies are well trained within their designated cost limits.

**Attack Baselines.** We treat L2 attacks as stronger-assumption baselines (upper bounds) to contextualize the effectiveness of our L1 framework under realistic access constraints. We compare our method with the following attack baselines:

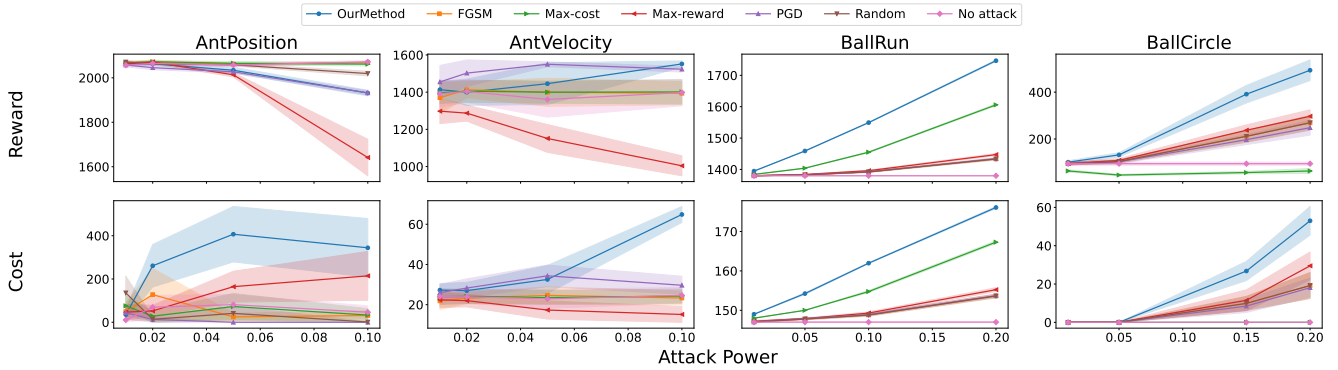


Figure 2: Adversarial attack results across four environments. Top row: reward curves. Bottom row: cost curves. From left to right: AntPosition, AntVelocity, BallRun, BallCircle. Our method (blue line) achieves consistently strong safety violations under L1 assumptions compared to all baselines that require gradient access (L2).

Table 2: Expert policy evaluation results. Reward and cost are averaged over evaluation episodes.

Environment	Avg. Reward	Avg. Cost
Safe-Ant-Velocity	$1397.71 \pm 106.35$	$23.60 \pm 5.94$
Safe-Ant-Position	$2066.06 \pm 13.50$	$77.90 \pm 152.78$
SafetyBallRun	$1368.9 \pm 0.3$	$146.0 \pm 0.0$
SafetyBallCircle	$91.9 \pm 13.4$	$0.0 \pm 0.0$

Table 3: ICRL learner policy evaluation results (50 episodes). Reward and cost are averaged over evaluation episodes.

Environment	Avg. Reward	Avg. Cost
Safe-Ant-Velocity	$1341.94 \pm 205.75$	$22.70 \pm 10.56$
Safe-Ant-Position	$2068.08 \pm 12.30$	$61.42 \pm 117.89$
SafetyBallRun	$5019.18 \pm 47.38$	$240.52 \pm 0.88$
SafetyBallCircle	$534.23 \pm 42.86$	$117.96 \pm 13.75$

**FGSM Attacker (L2):** This method [Goodfellow *et al.*, 2014] uses the gradient of the target critic network,  $grad = \nabla_s J(s, \pi^{target})$ , along with uniform noise to iteratively perturb the state. If the perturbed state induces an undesirable action, it is stored as an adversarial sample.

**PGD Attacker (L2):** This method [Pattanaik *et al.*, 2017] uses gradient information from the target critic to generate perturbations via projected gradient descent.

**Max-Reward Attacker (L2):** This attacker [Liu *et al.*, 2022b] optimizes perturbations to maximize the reward critic of the victim policy to guide the policy toward constraint violations. The loss is  $l = -\|q_r\|$ , where  $q_r$  is the reward critic.

**Max-Cost Attacker (L2):** This attacker [Liu *et al.*, 2022b] maximizes the cost critic of the victim policy. The loss is  $l = -\|q_c\|$ , where  $q_c$  is the cost critic.

Note that **(L2)** methods require privileged access to the expert policy’s gradients, while our method **(L1)** requires only trajectories and black-box interaction—no victim gradients or ground-truth constraints.

## 5.2 ICRL Results

To train the ICRL algorithm, we first collect 100 episodes of expert demonstrations from each environment. The ICRL training additionally requires black-box interaction with the environment to optimize the learner policy; we perform 20–50 epochs of policy updates depending on the environment. Importantly, this interaction does not require access to victim gradients or ground-truth constraints. This setting reflects a practical attack scenario.

For Safe-Ant-Velocity, we train the ICRL algorithm for 20 epochs for the outer constrained RL policy learner and 10 epochs for the inner constraint learner. For Safe-Ant-Position, the training setup is similar, except that the inner constraint learner runs for 50 epochs.

For the SafetyBallRun and SafetyBallCircle environments, we train ICRL using 50 epochs for the outer policy optimization loop and 10 epochs for the inner constraint learning loop.

Table 3 summarizes the ICRL learner policy performance. Comparing with the expert policy results in Table 2, the ICRL learner policies achieve comparable rewards. However, since we do not filter demonstrations, the ICRL learner policies achieve higher costs than the expert policies.

## 5.3 Attack Results

We evaluate all attacks on four environments with 50 episodes per setting (mean $\pm$ std). We sweep perturbation budgets  $\epsilon \in \{0.01, 0.02, 0.05, 0.1\}$  for Ant tasks and  $\epsilon \in \{0.05, 0.1, 0.15, 0.2\}$  for Ball tasks.

Overall, our method consistently induces larger safety violations than baseline attacks, while preserving comparable returns, despite requiring only trajectories and black-box interaction (L1). In Safe-Ant-Position, our attack increases the episode cost up to  $\sim 500$  at  $\epsilon = 0.1$ , whereas all baselines remain below 150. In Safe-Ant-Velocity, our method reaches cost  $> 65$  at  $\epsilon = 0.1$ , compared to  $< 40$  for all baselines. For SafetyBallRun, our method performs comparably to the max-cost baseline at high budgets (cost  $\sim 180$  at  $\epsilon = 0.2$ ), suggesting that reward-driven behaviors can overlap with unsafe behaviors. For SafetyBallCircle, our method achieves substantially higher cost (around 70 at  $\epsilon = 0.2$ ), outperforming weaker baselines and showing clear attack effectiveness.

Table 4: Generalization to max-cost attack method. We compare ground-truth (GT) based attacks versus ICRL-learned attacks across different environments. Cost values shown with violation rates in parentheses.

Env	$\epsilon$	GT-based Attack			ICRL-based Attack		
		Cost	Return	Viol. %	Cost	Return	Viol. %
BallCircle	0.05	0.0	109.9 $\pm$ 0.9	0.0%	0.0	31.7 $\pm$ 0.6	0.0%
	0.10	0.0	167.3 $\pm$ 2.0	0.0%	0.0	22.3 $\pm$ 0.6	0.0%
	0.20	2.4 $\pm$ 0.3	339.5 $\pm$ 4.9	0.0%	0.0	24.4 $\pm$ 1.3	0.0%
	0.30	8.1 $\pm$ 0.7	414.2 $\pm$ 7.7	6.0%	2.2 $\pm$ 0.4	63.6 $\pm$ 6.4	0.7%
BallRun	0.01	147.0	1639.7 $\pm$ 0.1	100%	142.0	1580.3 $\pm$ 0.0	100%
	0.05	151.9 $\pm$ 0.0	1694.3 $\pm$ 0.6	100%	134.1 $\pm$ 0.0	1461.2 $\pm$ 0.1	100%
	0.10	158.2 $\pm$ 0.1	1775.0 $\pm$ 1.3	100%	133.2 $\pm$ 0.1	1430.5 $\pm$ 0.8	100%
	0.20	171.3 $\pm$ 0.1	1957.3 $\pm$ 0.8	100%	156.4 $\pm$ 0.1	1634.9 $\pm$ 0.7	100%
Ant-Position	0.01	87.9 $\pm$ 150.1	2063.6 $\pm$ 19.3	64%	68.3 $\pm$ 126.8	2064.3 $\pm$ 11.5	50%
	0.02	76.7 $\pm$ 164.4	2068.0 $\pm$ 13.3	64%	42.2 $\pm$ 56.4	2062.5 $\pm$ 18.3	66%
	0.05	66.1 $\pm$ 130.9	2069.3 $\pm$ 13.7	66%	45.2 $\pm$ 117.0	2061.0 $\pm$ 11.7	54%
	0.10	82.9 $\pm$ 164.0	2067.4 $\pm$ 12.4	66%	47.3 $\pm$ 91.6	2064.3 $\pm$ 14.3	52%
Ant-Velocity	0.01	25.4 $\pm$ 6.3	1420.4 $\pm$ 88.2	100%	23.1 $\pm$ 7.9	1386.9 $\pm$ 157.1	100%
	0.02	22.9 $\pm$ 6.3	1389.7 $\pm$ 115.1	100%	23.8 $\pm$ 9.2	1387.1 $\pm$ 166.1	100%
	0.05	24.4 $\pm$ 6.7	1392.7 $\pm$ 132.6	100%	25.3 $\pm$ 6.1	1414.2 $\pm$ 84.7	100%
	0.10	23.3 $\pm$ 7.4	1392.0 $\pm$ 145.5	100%	24.8 $\pm$ 5.7	1422.4 $\pm$ 83.6	100%

#### 5.4 Generalization to Max-Cost Attacks

To demonstrate that our ICRL attack framework generalizes beyond our proposed attack method, we evaluate its applicability to the max-cost attack (which requires cost-critic gradients). We test across four environments: SafetyBallCircle, SafetyBallRun, SafetyAnt-Position, and SafetyAnt-Velocity. We compare attacks using ground-truth (GT) constraint information versus our ICRL-learned constraint network.

Table 4 presents the results. Overall, GT-based attacks achieve higher cost values than ICRL-based attacks. For example, in SafetyBallRun, GT achieves costs of 147-171 compared to ICRL’s 133-156 across different  $\epsilon$  values; in SafetyAnt-Position, GT reaches costs of 66-88 while ICRL achieves 42-68. Meanwhile, our ICRL-learned constraint network also provides effective guidance for attacks and achieves notable attack performance. For instance, in SafetyAnt-Velocity, ICRL-based attacks achieve costs of 23-25, nearly matching GT’s performance. In SafetyBallCircle at  $\epsilon = 0.30$ , ICRL successfully induces cost violations (2.2) following GT’s trend (8.1). In summary, our ICRL-based attack framework can generalize to other attack methods such as max-cost attack, effectively inducing cost violations across diverse environments. This demonstrates the generalization capability of our proposed framework.

#### 5.5 Determining Attack Strength

A key challenge in adversarial attacks on Safe RL agents is determining an appropriate attack strength that reliably induces safety violations without compromising stealth. If perturbations are too small, the induced constraint cost may be negligible. Conversely, overly large perturbations risk being

easily detected.

As shown in Lemma 3, the increase in episodic cost is controlled by the Lipschitz continuity of the constraint function  $\psi$  and system dynamics, providing a principled link between the attack budget  $\epsilon$  and resulting cost violations. In practice, we evaluated with 100 epochs of expert trajectories on Safe-Ant-Velocity. The estimated Lipschitz constants were  $L_\psi \in \{0.0829, 0.1262, 0.1072, 0.1366\}$ . Substituting these into Lemma 3, we obtained theoretical upper bounds  $\{179.39, 231.58, 217.93, 238.39\}$ , all safely exceeding the observed costs  $\{42.08, 62.05, 141.05, 119.69\}$ . This confirms that Lemma 3 provides valid and practical upper bounds. Conversely, given a predefined cost value, we can calculate the required attack strength.

#### 6 Defense

Our method exposes the vulnerability of safe RL policies to adversarial attacks. Equally important is the need to enhance the robustness of these policies against such attacks. One effective strategy is adversarial training, which incorporates adversarial perturbations into the training process to improve the policy’s resilience. Another promising approach is probabilistic shielding [Belardinelli *et al.*, 2025], which identifies and prevents actions that are likely to violate safety constraints. Furthermore, as discussed in the limitations, explicitly encoding safety constraints in the state representation can significantly reduce the success rate of our attack.

#### 7 Conclusion

In this work, we proposed an adversarial attack framework that addresses key challenges in analyzing vulnerabilities of

safe reinforcement learning (Safe RL) policies. First, our method leverages trajectories and black-box interaction to conduct attacks without requiring privileged access to victim gradients or ground-truth constraints, making it practical under realistic access constraints. Second, by leveraging the safety constraint network and learner policy obtained via ICRL, it can estimate the expected cost bound and set the attack budget accordingly. Finally, the framework provides a systematic way to study the vulnerabilities and robustness of Safe RL policies, offering new insights for developing safer learning systems.

## References

[Belardinelli *et al.*, 2025] Francesco Belardinelli, Alexander W Goodall, et al. Probabilistic shielding for safe reinforcement learning. In *Proceedings of the AAAI Conference on Artificial Intelligence*, volume 39, pages 16091–16099, 2025.

[Brunke *et al.*, 2022] Lukas Brunke, Melissa Greeff, Adam W Hall, Zhaocong Yuan, Siqi Zhou, Jacopo Panerati, and Angela P Schoellig. Safe learning in robotics: From learning-based control to safe reinforcement learning. *Annual Review of Control, Robotics, and Autonomous Systems*, 5(1):411–444, 2022.

[Bui *et al.*, 2024] Van-Hai Bui, Srijita Das, Akhtar Hussain, Guilherme Vieira Hollweg, and Wencong Su. A critical review of safe reinforcement learning techniques in smart grid applications. *arXiv preprint arXiv:2409.16256*, 2024.

[Ellenberger, 2018 2019] Benjamin Ellenberger. Pybullet gymperium. <https://github.com/benelot/pybullet-gym>, 2018–2019.

[Goodfellow *et al.*, 2014] Ian J Goodfellow, Jonathon Shlens, and Christian Szegedy. Explaining and harnessing adversarial examples. *arXiv preprint arXiv:1412.6572*, 2014.

[Gu *et al.*, 2022] Shangding Gu, Long Yang, Yali Du, Guang Chen, Florian Walter, Jun Wang, and Alois Knoll. A review of safe reinforcement learning: Methods, theory and applications. *arXiv preprint arXiv:2205.10330*, 2022.

[Huang *et al.*, 2017] Sandy Huang, Nicolas Papernot, Ian Goodfellow, Yan Duan, and Pieter Abbeel. Adversarial attacks on neural network policies. *arXiv preprint arXiv:1702.02284*, 2017.

[Hugessen *et al.*, 2024] Adriana Hugessen, Harley Wiltzer, and Glen Berseth. Simplifying constraint inference with inverse reinforcement learning. In *The Thirty-eighth Annual Conference on Neural Information Processing Systems*, 2024.

[Ji *et al.*, 2024] Jiaming Ji, Jiayi Zhou, Borong Zhang, Juntao Dai, Xuehai Pan, Ruiyang Sun, Weidong Huang, Yiran Geng, Mickel Liu, and Yaodong Yang. Omnisafe: An infrastructure for accelerating safe reinforcement learning research. *Journal of Machine Learning Research*, 25(285):1–6, 2024.

[Jiang *et al.*, 2024] Shixiong Jiang, Mengyu Liu, and Fanxin Kong. Vulnerability analysis for safe reinforcement learning in cyber-physical systems. In *2024 ACM/IEEE 15th International Conference on Cyber-Physical Systems (IC-CPS)*, pages 77–86. IEEE, 2024.

[Kim *et al.*, 2024] Konwoo Kim, Gokul Swamy, Zuxin Liu, Ding Zhao, Sanjiban Choudhury, and Steven Z Wu. Learning shared safety constraints from multi-task demonstrations. *Advances in Neural Information Processing Systems*, 36, 2024.

[Liang *et al.*, 2022] Yongyuan Liang, Yanchao Sun, Ruijie Zheng, and Furong Huang. Efficient adversarial training without attacking: Worst-case-aware robust reinforcement learning. *Advances in Neural Information Processing Systems*, 35:22547–22561, 2022.

[Lin *et al.*, 2017] Yen-Chen Lin, Zhang-Wei Hong, Yuan-Hong Liao, Meng-Li Shih, Ming-Yu Liu, and Min Sun. Tactics of adversarial attack on deep reinforcement learning agents. *arXiv preprint arXiv:1703.06748*, 2017.

[Lindner *et al.*, 2024] David Lindner, Xin Chen, Sebastian Tschiatschek, Katja Hofmann, and Andreas Krause. Learning safety constraints from demonstrations with unknown rewards. In *International Conference on Artificial Intelligence and Statistics*, pages 2386–2394. PMLR, 2024.

[Liu *et al.*, 2022a] Guiliang Liu, Yudong Luo, Ashish Gaurav, Kasra Rezaee, and Pascal Poupart. Benchmarking constraint inference in inverse reinforcement learning. *arXiv preprint arXiv:2206.09670*, 2022.

[Liu *et al.*, 2022b] Zuxin Liu, Zijian Guo, Zhepeng Cen, Huan Zhang, Jie Tan, Bo Li, and Ding Zhao. On the robustness of safe reinforcement learning under observational perturbations. *arXiv preprint arXiv:2205.14691*, 2022.

[Madry *et al.*, 2018] Aleksander Madry, Aleksandar Makelov, Ludwig Schmidt, Dimitris Tsipras, and Adrian Vladu. Towards deep learning models resistant to adversarial attacks. In *International Conference on Learning Representations*, 2018.

[Malik *et al.*, 2021] Shehryar Malik, Usman Anwar, Alireza Aghasi, and Ali Ahmed. Inverse constrained reinforcement learning. In *International conference on machine learning*, pages 7390–7399. PMLR, 2021.

[McPherson *et al.*, 2021] David L McPherson, Kaylene C Stocking, and S Shankar Sastry. Maximum likelihood constraint inference from stochastic demonstrations. In *2021 IEEE Conference on Control Technology and Applications (CCTA)*, pages 1208–1213. IEEE, 2021.

[Pattanaik *et al.*, 2017] Anay Pattanaik, Zhenyi Tang, Shuijing Liu, Gautham Bommannan, and Girish Chowdhary. Robust deep reinforcement learning with adversarial attacks. *arXiv preprint arXiv:1712.03632*, 2017.

[Qiao *et al.*, 2024] Guanren Qiao, Guiliang Liu, Pascal Poupart, and Zhiqiang Xu. Multi-modal inverse constrained reinforcement learning from a mixture of demon-

strations. *Advances in Neural Information Processing Systems*, 36, 2024.

[Ray *et al.*, 2019] Alex Ray, Joshua Achiam, and Dario Amodei. Benchmarking safe exploration in deep reinforcement learning. *arXiv preprint arXiv:1910.01708*, 7(1):2, 2019.

[Scobee and Sastry, 2019] Dexter RR Scobee and S Shankar Sastry. Maximum likelihood constraint inference for inverse reinforcement learning. *arXiv preprint arXiv:1909.05477*, 2019.

[Stooke *et al.*, 2020] Adam Stooke, Joshua Achiam, and Pieter Abbeel. Responsive safety in reinforcement learning by pid lagrangian methods. In *International Conference on Machine Learning*, pages 9133–9143. PMLR, 2020.

[Wachi *et al.*, 2024] Akifumi Wachi, Xun Shen, and Yanan Sui. A survey of constraint formulations in safe reinforcement learning. *arXiv preprint arXiv:2402.02025*, 2024.

[Xu and Liu, ] Sheng Xu and Guiliang Liu. Robust inverse constrained reinforcement learning under model misspecification. In *Forty-first International Conference on Machine Learning*.

[Yifru and Baheri, 2024] Lunet Yifru and Ali Baheri. Concurrent learning of control policy and unknown safety specifications in reinforcement learning. *IEEE Open Journal of Control Systems*, 2024.

[Zhang *et al.*, 2020] Huan Zhang, Hongge Chen, Chaowei Xiao, Bo Li, Mingyan Liu, Duane Boning, and Cho-Jui Hsieh. Robust deep reinforcement learning against adversarial perturbations on state observations. *Advances in Neural Information Processing Systems*, 33:21024–21037, 2020.

## 8 Proof of Theorems

### 8.1 Proof of Theorem 1

*Proof.* By the uniform approximation bound, we have

$$|\psi(s, a) - \psi^*(s, a)| \leq \epsilon \Rightarrow \psi^*(s, a) \geq \psi(s, a) - \epsilon.$$

Substituting  $(s + \delta_s, \pi_E(s + \delta_s))$  into the above, we get

$$\psi^*(s + \delta_s, \pi_E(s + \delta_s)) \geq \psi(s + \delta_s, \pi_E(s + \delta_s)) - \epsilon > \delta - \epsilon.$$

Therefore, the perturbed state-action pair results in a violation of the true constraint when  $\delta > \epsilon$ .  $\square$

### 8.2 Proof of Lemma 1

*Proof.* We prove local optimality by contradiction. Assume, for the sake of contradiction, that there exists another perturbation  $\hat{\delta}$  with  $\|\hat{\delta}\| \leq \epsilon$  in a local neighborhood of  $s$ , such that:

$$\psi(s + \hat{\delta}, \pi_E(s + \hat{\delta})) > \psi(s + \delta^*, \pi_E(s + \delta^*)).$$

Since  $\psi(s, a)$  is differentiable with respect to  $s$ , we have the first-order Taylor expansion around the point  $(s, \pi_E(s))$ :

$$\psi(s + \hat{\delta}, \pi_E(s + \hat{\delta})) \approx \psi(s, \pi_E(s)) + \nabla_s \psi(s, \pi_E(s))^\top \hat{\delta}.$$

The perturbation  $\delta^*$  defined by projected gradient ascent maximizes the linear approximation:

$$\delta^* = \arg \max_{\|\delta\| \leq \epsilon} \nabla_s \psi(s, \pi_E(s))^\top \delta.$$

By the definition of the maximization, we have:

$$\nabla_s \psi(s, \pi_E(s))^\top \hat{\delta} \leq \nabla_s \psi(s, \pi_E(s))^\top \delta^*.$$

This implies:

$$\psi(s + \hat{\delta}, \pi_E(s + \hat{\delta})) \leq \psi(s, \pi_E(s)) + \nabla_s \psi(s, \pi_E(s))^\top \delta^*.$$

But from the Taylor approximation for  $\delta^*$ , we also have:

$$\psi(s + \delta^*, \pi_E(s + \delta^*)) \approx \psi(s, \pi_E(s)) + \nabla_s \psi(s, \pi_E(s))^\top \delta^*.$$

Therefore, we must have:

$$\psi(s + \hat{\delta}, \pi_E(s + \hat{\delta})) \leq \psi(s + \delta^*, \pi_E(s + \delta^*)),$$

which directly contradicts our initial assumption. Thus, there is no perturbation in a local neighborhood around  $s$  that achieves higher constraint violation than the gradient-based perturbation  $\delta^*$ . Hence, the gradient-based perturbation is locally optimal.  $\square$

### 8.3 Proof of Lemma 2

*Proof.* By definition of Lipschitz continuity, we have:

$$|\psi(s + \delta, a) - \psi(s, a)| \leq L_\psi \|\delta\|.$$

Substituting  $a = \pi_E(s + \delta)$ , and noting  $\|\delta\| \leq \epsilon$ , we immediately obtain:

$$\psi(s + \delta, \pi_E(s + \delta)) \leq \psi(s, \pi_E(s)) + L_\psi \epsilon.$$

Further noting that policy  $\pi_E$  is stationary and locally continuous, we have that, in a sufficiently small local neighborhood,

$$|\psi(s, \pi_E(s + \delta)) - \psi(s, \pi_E(s))| \approx 0,$$

thus arriving at the simpler bound:

$$\psi(s + \delta, \pi_E(s + \delta)) \leq \psi(s, \pi_E(s)) + L_\psi \epsilon.$$

This completes the proof.  $\square$

### 8.4 Proof of Lemma 3

*Proof.* We start from the Lipschitz continuity assumption:

$$\begin{aligned} |\psi(s_t + \delta_t, \pi_E(s_t + \delta_t)) - \psi(s_t, \pi_E(s_t))| &\leq L_\psi \|s_t + \delta_t - s_t\| \\ &= L_\psi \|\delta_t\| \leq L_\psi \epsilon. \end{aligned}$$

Thus, at each step  $t$ , we have the following bound:

$$\psi(s_t + \delta_t, \pi_E(s_t + \delta_t)) \leq \psi(s_t, \pi_E(s_t)) + L_\psi \epsilon.$$

Now, note that the perturbation at each time-step affects subsequent states through system dynamics. Assuming the system dynamics are Lipschitz continuous with constant  $L_f$ , we have:

$$\|s_{t+1} - \hat{s}_{t+1}\| \leq L_f \|s_t + \delta_t - s_t\| \leq L_f \epsilon,$$

where  $\hat{s}_{t+1}$  denotes the state without perturbation at time  $t + 1$ .

Iteratively applying this logic, at time step  $t$ , the perturbation effect accumulates as:

$$\|s_t + \delta_t - s_t\| \leq L_f^{t-1} \epsilon.$$

Thus, the episodic cumulative constraint cost under perturbation satisfies:

$$\sum_{t=1}^T \psi(s_t + \delta_t, \pi_E(s_t + \delta_t)) \leq \sum_{t=1}^T \psi(s_t, \pi_E(s_t)) + L_\psi \epsilon \sum_{t=1}^T L_f^{t-1}.$$

The geometric series on the right side can be simplified as:

$$\sum_{t=1}^T L_f^{t-1} = \frac{1 - L_f^T}{1 - L_f}.$$

Thus, we have the final bound:

$$\sum_{t=1}^T \psi(s_t + \delta_t, \pi_E(s_t + \delta_t)) \leq \sum_{t=1}^T \psi(s_t, \pi_E(s_t)) + \frac{L_\psi \epsilon (1 - L_f^T)}{1 - L_f}.$$

This concludes the proof.  $\square$

## 9 Implementation Details

### 9.1 System Identification

To estimate the next state  $s_{t+1}$  and compute state gradients, we perform system identification by training a multi-layer perceptron (MLP) on expert trajectories. Given  $(s_t, a_t, s_{t+1})$  tuples collected from the expert policy  $\pi_E$ , the MLP learns the mapping

$$s_{t+1} = \hat{f}(s_t, a_t). \quad (6)$$

This learned model  $\hat{f}$  serves two purposes: (i) predicting the next state  $s_{t+1}$  for adversarial attack generation, and (ii) providing a differentiable approximation that allows computing  $\nabla_{s'_t} c(\hat{f}(s'_t, \pi(s'_t)))$  in Algorithm 1.

Taking the Safe-Ant-Velocity environment as an example, we collect 100 epochs of trajectories (100,000 steps) under the expert policy. The MLP is trained on these data and evaluated on 50 unseen trajectories, achieving a mean squared error (MSE) of 0.000672, which demonstrates high predictive accuracy. Despite being approximate, the learned dynamics captures local transition behavior effectively, enabling reliable gradient-based perturbation generation without assuming access to the true dynamics.